EUROPEAN ORGANIZATION FOR NUCLEAR RESEARCH

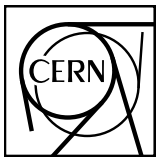

ALICE-ANA-2016-xxx
November 30, 2016

Lambda-Kaon and Cascade-Kaon Femtoscopy in Pb-Pb Collisions at $\sqrt{s_{NN}} = 2.76$ TeV from the LHC ALICE Experiment

Jesse T. Buxton[1]

1. Department of Physics, The Ohio State University, Columbus, Ohio, USA

Email: jesse.thomas.buxton@cern.ch

Abstract

We present results from a femtoscopic analysis of Lambda-Kaon correlations in Pb-Pb collisions at $\sqrt{s_{NN}}$ = 2.76 TeV by the ALICE experiment at the LHC. All pair combinations of Λ and $\bar{\Lambda}$ with K^+, K^- and K^0_S are analyzed. The femtoscopic correlations are the result of strong final-state interactions, and are fit with a parametrization based on a model by R. Lednicky and V. L. Lyuboshitz[1]. This allows us to both characterize the emission source and measure the scattering parameters for the particle pairs. We observe a large difference in the Λ-K^+ ($\bar{\Lambda}$-K^-) and Λ-K^- ($\bar{\Lambda}$-K^+) correlations in pairs with low relative momenta (k* $\lesssim$ 100 MeV). Additionally, the average of the Λ-K^+ ($\bar{\Lambda}$-K^-) and Λ-K^- ($\bar{\Lambda}$-K^+) correlation functions is consistent with our Λ-K^0_S ($\bar{\Lambda}$-K^0_S) measurement. The results suggest an effect arising from different quark-antiquark interactions in the pairs, i.e. $s\bar{s}$ in Λ-K^+ ($\bar{\Lambda}$-K^-) and $u\bar{u}$ in Λ-K^- ($\bar{\Lambda}$-K^+). To gain further insight into this hypothesis, we currently are conducting a Cascade-Kaon femtoscopic analysis.

Contents

List of Figures

1 Introduction

This will be my introduction. Remember, Jai suggested to make each sentence a separate line to make changes easier to track in git. Otherwise, git will treat an entire paragraph as a single line!

And a new paragraph begins with an empty line.

2 Data Sample and Software

2.1 Data Sample

The analysis used "pass 2" reconstructed Pb-Pb data from LHC11h (AOD145). The runlist was selected from runs with global quality tag "1" in the ALICE Run Condition Table. Approximately 40 million combined central, semi-central, and minimum bias events were analyzed. Runs from both positive (++) and negative (--) magnetic field polarity settings were used.

Run list: 170593, 170572, 170388, 170387, 170315, 170313, 170312, 170311, 170309, 170308, 170306, 170270, 170269, 170268, 170230, 170228, 170207, 170204, 170203, 170193, 170163, 170159, 170155, 170091, 170089, 170088, 170085, 170084, 170083, 170081, 170040, 170027, 169965, 169923, 169859, 169858, 169855, 169846, 169838, 169837, 169835, 169591, 169590, 169588, 169587, 169586, 169557, 169555, 169554, 169553, 169550, 169515, 169512, 169506, 169504, 169498, 169475, 169420, 169419, 169418, 169417, 169415, 169411, 169238, 169167, 169160, 169156, 169148, 169145, 169144, 169138, 169099, 169094, 169091, 169045, 169044, 169040, 169035, 168992, 168988, 168826, 168777, 168514, 168512, 168511, 168467, 168464, 168460, 168458, 168362, 168361, 168342, 168341, 168325, 168322, 168311, 168310, 168115, 168108, 168107, 168105, 168076, 168069, 167988, 167987, 167985, 167920, 167915

Analysis was also performed on the LHC12a17a_fix (AOD149) Monte Carlo HIJING events for certain checks.

2.2 Software

The analysis was performed on the PWGCF analysis train using AliRoot v5-08-18-1 and AliPhysics vAN-20161027-1.

The main classes utilized include: AliFemtoVertexMultAnalysis, AliFemtoEventCutEstimators, AliFemtoESDTrackCutNSigmaFilter, AliFemtoV0TrackCutNSigmaFilter, AliFemtoXiTrackCut, AliFemtoV0PairCut, AliFemtoV0TrackPairCut, AliFemtoXiTrackPairCut, and AliFemtoAnalysisLambdaKaon. All of these classes are contained in /AliPhysics/PWGCF/FEMTOSCOPY/AliFemto and .../AliFemtoUser.

3 Data Selection

3.1 Event Selection and Mixing

The events used in this study were selected with the class AliFemtoEventCutEstimators according to the following criteria:

- Triggers
  - minimum bias (kMB)
  - central (kCentral)
  - semi-central (kSemiCentral)
- z-position of reconstructed event vertex must be within 10 cm of the center of the ALICE detector

– the event must contain at least one particle of each type from the pair of interest

The event mixing was handled by the AliFemtoVertexMultAnalysis class, which only mixes events with like vertex position and centrality. The following criteria were used for event mixing:

– Number of events to mix = 5
– Vertex position bin width = 2 cm
– Centrality bin width = 5

The AliFemtoEventReaderAODChain class is used to read the events. Event flatteneing is not currently used. FilterBit(7). The centrality is determined by the "V0M" method of AliCentrality, set by calling AliFemtoEventReaderAOD::SetUseMultiplicity(kCentrality). I utilize the SetPrimaryVertexCorrectionTPCPoints switch, which causes the reader to shift all TPC points to be relative to the event vertex.

3.2 $K^{\pm}$ Track Selection

Charged kaons are identified using the AliFemtoESDTrackCutNSigmaFilter class. The specific cuts used in this analysis are as follows:

Track Selection:

– Kinematic range:
  – $0.14 < p_T < 1.5$
  – $|\eta| < 0.8$
– FilterBit8
  – TPC tracks
– Track Quality
  – Minimum number of clusters in the TPC (fminTPCncls) = 80
  – Maximum allowed χ^2/N_{DOF} for ITS clusters = 3.0
  – Maximum allowed χ^2/N_{DOF} for TPC clusters = 4.0
– Primary Particle Selection:
  – Maximum XY impact parameter = 2.4
  – Maximum Z impact parameter = 3.0
– Remove particles with any kink labels (fRemoveKinks = true)
– Maximum allowed sigma to primary vertex (fMaxSigmaToVertex) = 3.0

$K^{\pm}$ Identification:

– PID Probabilities:
  – K: > 0.2
  – π: < 0.1
  – μ: < 0.8

  - p: < 0.1
- Most probable particle type must be Kaon (fMostProbable=3)
- TPC and TOF N_σ cuts:
  - p < 0.4 GeV/c: $N_{\sigma K,TPC} < 2$
  - $0.4 <$ p < 0.45 GeV/c: $N_{\sigma K,TPC} < 1$
  - $0.45 <$ p < 0.8 GeV/c: $N_{\sigma K,TPC} < 3$ & $N_{\sigma K,TOF} < 2$
  - $0.8 <$ p < 1.0 GeV/c: $N_{\sigma K,TPC} < 3$ & $N_{\sigma K,TOF} < 1.5$
  - p > 1.0 GeV/c: $N_{\sigma K,TPC} < 3$ & $N_{\sigma K,TOF} < 1$
- Electron Rejection: Reject if $N_{\sigma e-,TPC} < 3$
- Pion Rejection: Reject if:
  - p < 0.65
    - if TOF and TPC available: $N_{\sigma \pi,TPC} < 3$ & $N_{\sigma \pi,TOF} < 3$
    - else
      - p < 0.5: $N_{\sigma \pi,TPC} < 3$
      - $0.5 <$ p < 0.65: $N_{\sigma \pi,TPC} < 2$
  - $0.65 <$ p < 1.5: $N_{\sigma \pi,TPC} < 5$ & $N_{\sigma \pi,TOF} < 3$
  - p > 1.5: $N_{\sigma \pi,TPC} < 5$ & $N_{\sigma \pi,TOF} < 2$

The purity of the $K^\pm$ collections was estimated using the MC data, for which the true identity of each reconstructed $K^\pm$ particle is known. Therefore, the purity may be estimated as:

$$Purity(K^\pm) = \frac{N_{true}}{N_{reconstructed}} \tag{1}$$

Purity(K^+) $\approx$ Purity(K^-) $\approx 97\%$

3.3 V0 Selection

Λ ($\bar{\Lambda}$) and K^0_S are neutral particles which cannot be directly detected, but must instead be reconstructed through detection of their decay products, or daughters. This process is illustrated in Figure 1. In general, particles which are topologically reconstructed in this fashion are called V0 particles. The class AliFemtoV0TrackCutNSigmaFilter (which is an extension of AliFemtoV0TrackCut) is used to reconstruct the V0s.

3.3.1 Λ Reconstruction

The following cuts were used to select good Λ ($\bar{\Lambda}$) candidates:

1. Daughter Particle Cuts
   (a) Cuts Common to Both Daughters
      i. $|\eta| < 0.8$
      ii. SetTPCnclsDaughters(80)
      iii. SetStatusDaughters(AliESDtrack::kTPCrefic)
      iv. SetMaxDcaV0Daughters(0.4)

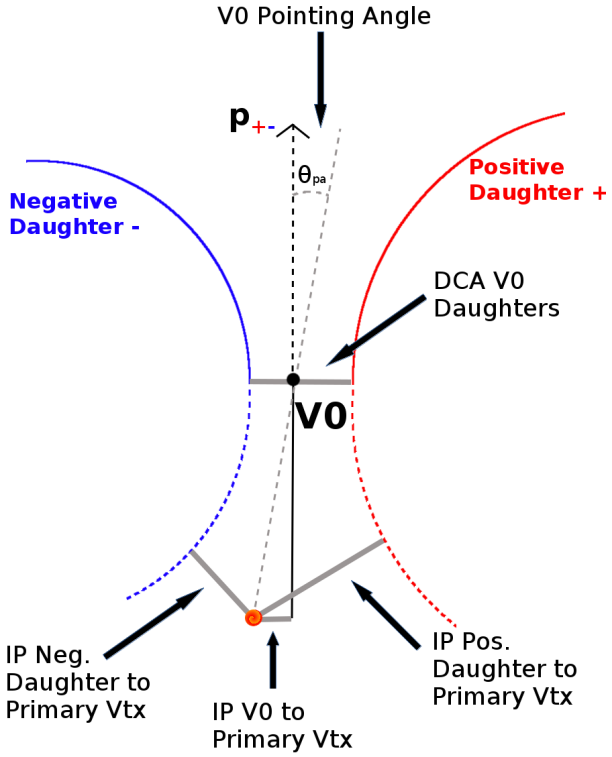

Fig. 1: V0 Reconstruction

(b) Pion Specific Daughter Cuts

i. $p_T > 0.16$

ii. DCA to prim vertex > 0.3

(c) Proton Specific Daughter Cuts

i. $p_T > 0.5(p)$ [$0.3(\bar{p})$] GeV/c

ii. DCA to prim vertex > 0.1

2. V0 Cuts

(a) $|\eta| < 0.8$

(b) $p_T > 0.4$

(c) $|m_{inv} - m_{PDG}| < 3.8$ MeV

(d) Cosine of pointing angle > 0.9993

(e) OnFlyStatus = false

(f) Decay Length < 60 cm

3.3.2 K^0_S Reconstruction

The following cuts were used to select good K^0_S candidates:

1. Pion Daughter Cuts

(a) $|\eta| < 0.8$

(b) SetTPCnclsDaughters(80)

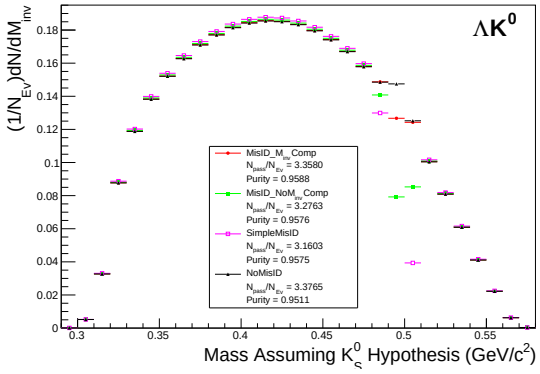

(a) Mass assuming K^0_S-hypothesis for Λ collection, i.e. assume the daughters are $\pi^+\pi^-$ instead of $p^+\pi^-$.

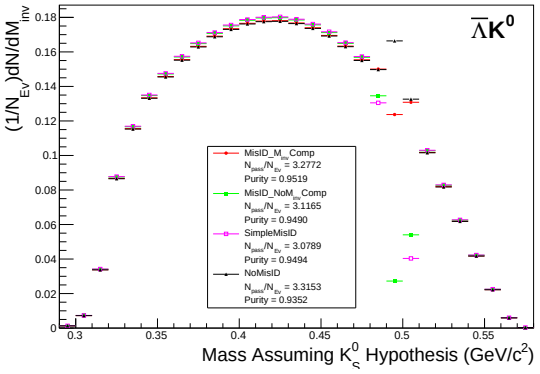

(b) Mass assuming K^0_S-hypothesis for $\bar{\Lambda}$ collection, i.e. assume the daughters are $\pi^+\pi^-$ instead of $\pi^+\bar{p}^-$.

Fig. 2: Mass assuming K^0_S-hypothesis for V0 candidates passing all Λ (2a) and $\bar{\Lambda}$ (2b) cuts. The "NoMisID" distribution (black triangles) uses the V0 finder without any attempt to remove misidentified K^0_S. The slight peak in the "NoMisID" distribution around $m_{inv} = 0.5$ GeV/c^2 likely contains misidentified K^0_S particles in our Λ collection. "SimpleMisID" (pink squares) simply cuts out the entire peak, which throws away some good Λ and $\bar{\Lambda}$ particles. "MisID_NoM$_{inv}$Comp" (green squares) uses the misidentification cut outlined in the text, but does not utilize the invariant mass comparison method. "MisID_M$_{inv}$Comp" (red circles) utilizes the full misidentification methods, and is currently used for this analysis. "N$_{pass}$/N$_{ev}$" is the total number of $\Lambda(\bar{\Lambda})$ particles found, normalized by the total number of events. The purity of the collection is also listed. If one simply cuts out the entire peak, good Λ particles will be lost. Ideally, the Λ selection and K^0_S misidentification cuts are selected such that the peak is removed from this plot while leaving the distribution continuous.

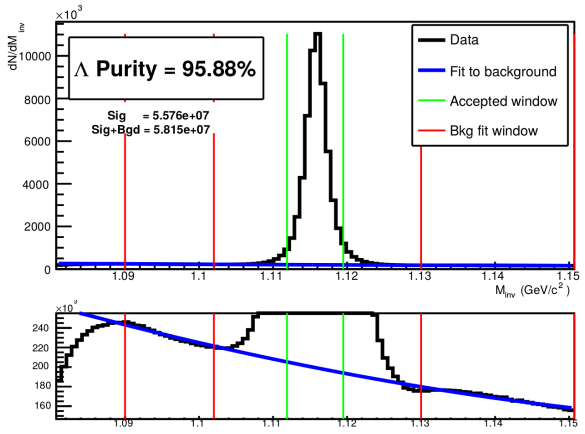

(a) Λ Purity

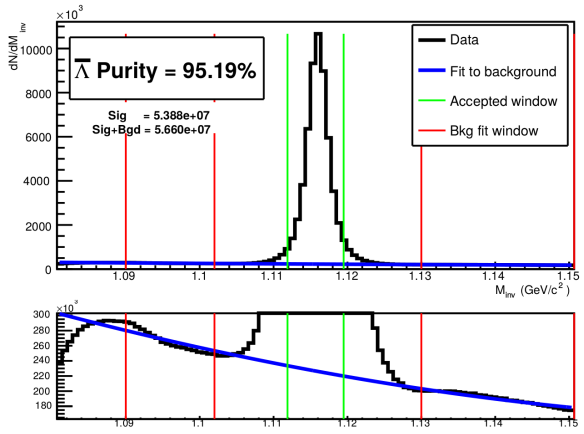

(b) $\bar{\Lambda}$ Purity

Fig. 3: Invariant mass (M$_{inv}$) distribution of all $\Lambda(\bar{\Lambda})$ candidates immediately before the final invariant mass cut. These distributions are used to calculate the collection purities, Purity(Λ) $\approx$ Purity($\bar{\Lambda}$) $\approx$ 95%.

(c) SetStatusDaughters(AliESDtrack::kTPCrefic)

(d) SetMaxDcaV0Daughters(0.3)

(e) $p_T > 0.15$

(f) DCA to prim vertex > 0.3

2. K^0_S Cuts

(a) $|\eta| < 0.8$

(b) $p_T > 0.2$

(c) $m_{PDG} - 13.677$ MeV $< m_{inv} < m_{PDG} + 2.0323$ MeV

(d) Cosine of pointing angle > 0.9993

(e) OnFlyStatus = false

(f) Decay Length < 30 cm

As can be seen in Figure 4, some misidentified Λ and $\bar{\Lambda}$ particles contaminate our K^0_S sample. Figure 4a shows the mass assuming Λ-hypothesis for the K^0_S collection, i.e. assume the daughters are $p^+\pi^-$ instead of $\pi^+\pi^-$. Figure 4b is similar, but shows the mass assuming $\bar{\Lambda}$ hypothesis for the collection, i.e. assume the daughters are $\pi^+\bar{p}^-$ instead of $\pi^+\pi^-$. The Λ contamination can be seen in 4a, and the $\bar{\Lambda}$ contamination in 4b, in the peaks around m_{inv} = 1.115 GeV/c^2. Additionally, the $\bar{\Lambda}$ contamination is visible in Figure 4a, and the Λ contamination visible in Figure 4b, in the region of excess around 1.65 $< m_{inv} <$ 2.1 GeV/c^2. This is confirmed as the number of misidentified Λ particles in the sharp peak of Figure 4a (misidentified $\bar{\Lambda}$ particles in the sharp peak of Figure 4b) approximately equals the excess found in the $1.65 < m_{inv} < 2.1$ GeV/c^2 region of Figure 4a (Figure 4b).

The peaks around $m_{inv} = 1.115$ GeV/c^2 in Figure 4 contain both misidentified Λ ($\bar{\Lambda}$) particles and good K^0_S. If one simply cuts out the entire peak, some good K^0_S particles will be lost. Ideally, the K^0_S selection and Λ($\bar{\Lambda}$) misidentification cuts can be selected such that the peak is removed from this plot while leaving the distribution continuous. To attempt to remove these Λ and $\bar{\Lambda}$ contaminations without throwing away good K^0_S particles, the following misidentification cuts are imposed; a K^0_S candidate is rejected if all of the following criteria are satisfied:

– $|m_{inv,\ \Lambda(\bar{\Lambda})\ Hypothesis} - m_{PDG,\ \Lambda(\bar{\Lambda})}| < 9.0$ MeV/c^2

– Positive daughter passes $p^+(\pi^+)$ daughter cut implemented for Λ($\bar{\Lambda}$) reconstruction

– Negative daughter passes $\pi^-(\bar{p}^-)$ daughter cut implemented by Λ($\bar{\Lambda}$) reconstruction

3.4 Cascade Reconstruction

Talk about reconstruction cascades

3.5 Pair Selection

Some general remarks on forming pairs

It is important to obtain true particle pairs in the analysis. In particular, contamination from pairs constructed with split or merged tracks can introduce an artificial signal into the correlation function, obscuring the actual physics.

4 Correlation Functions

This analysis studies the momentum correlations of both Λ-K and Ξ-K pairs using the two-particle correlation function, defined as $C(k^*) = A(k^*)/B(k^*)$, where $A(k^*)$ is the signal distribution, $B(k^*)$ is the reference (or background) distribution, and k^* is the momentum of one of the particles in the pair rest frame. In practice, $A(k^*)$ is constructed by binning in k^* pairs from the same event. Ideally, $B(k^*)$ is similar to $A(k^*)$ in all respects excluding the presence of femtoscopic correlations [1]; as such, $B(k^*)$ is used to divide out the phase-space effects, leaving only the femtoscopic effects in the correlation function.

In practice, $B(k^*)$ is obtained by forming mixed-event pairs, i.e. particles from a given event are paired with particles from N_{mix}(= 5) other events, and these pairs are then binned in k^*. In forming the background distribution, it is important to mix only similar events; mixing events with different phase-spaces can lead to artificial signals in the correlaton function. Therefore, in this analysis, we mix events with primary vertices within 2 cm and centralities within 5% of each other. Also note, a vertex correction is also applied to each event, which essentially recenters the the primary vertices to z = 0.

This analysis presents correlation functions for three centrality bins (0-10%, 10-30%, and 30-50%), and is currently pair transverse momentum ($k_T = 0.5|\mathbf{p}_{T,1} + \mathbf{p}_{T,2}|$) integrated (i.e. not binned in k_T). The correlation functions are constructed separately for the two magnetic field configurations, and are combined using a weighted average:

$$C_{combined}(k^*) = \frac{\sum_i w_i C_i(k^*)}{\sum_i w_i} \tag{2}$$

where the sum runs over the correlation functions to be combined, and the weight, w_i, is the number of numerator pairs in $C_i(k^*)$. Here, the sum is over the two field configurations.

Figures 9, 10, and 11 show the correlation functions for all centalities studied for $\Lambda K^0_S(\bar{\Lambda}K^0_S)$, $\Lambda K^+(\bar{\Lambda}K^-)$, and $\Lambda K^-(\bar{\Lambda}K^+)$, respectively.

5 Fitting

This section will include the Lednicky model and the method used to fit the Cascade study. It will also include momentum resolution, residual correlations, and any other aspects to obtain a good fit

5.1 Model: Lambda-Kaon

Talk about Lednicky model

$$\begin{aligned}
&C(k^*) = 1 + \lambda[\alpha \exp(-4k^{*2}R^2) + C_{FSI}(k^*)] \\
&C_{FSI}(k^*) = (1+\alpha)[\tfrac{1}{2}|\tfrac{f(k^*)}{R}|^2(1 - \tfrac{d_0}{2\sqrt{\pi}R}) + \tfrac{2\mathbb{R}f(k^*)}{\sqrt{\pi}R}F_1(2k^*R) - \tfrac{\mathbb{I}f(k^*)}{R}F_2(2k^*R)] \\
&f(k^*) = (\tfrac{1}{f_0} + \tfrac{1}{2}d_0k^{*2} - ik^*)^{-1}
\end{aligned} \tag{3}$$

5.2 Model: Cascade-Kaon

Talk about model

$$\begin{aligned}
&C(\mathbf{k}^*) = \sum_S \rho_S \int S(\mathbf{r}^*)|\Psi^S_{\mathbf{k}^*}(\mathbf{r}^*)|^2 d^3\mathbf{r}^* \\
&\Psi_{\mathbf{k}^*}(\mathbf{r}^*) = e^{i\delta_c}\sqrt{A_c(\eta)}[e^{i\mathbf{k}^*\cdot\mathbf{r}^*}F(-i\eta, 1, i\xi) + f_c(k^*)\tfrac{\tilde{G}(\rho,\eta)}{r^*}] \\
&f_c(k^*) = [\tfrac{1}{f_0} + \tfrac{1}{2}d_0k^{*2} - \tfrac{2}{a_c}h(\eta) - ik^*A_c(\eta)]^{-1} \\
&\rho = k^*r^*;\ \eta = (k^*a)^{-1};\ a = (\mu z_1 z_2 e^2)^{-1} \\
&\xi = \mathbf{k}^*\cdot\mathbf{r}^* + k^*r^* \equiv \rho(1+\cos\theta^*)
\end{aligned} \tag{4}$$

$$
\begin{aligned}
&C(\mathbf{k}^*) = \sum_S \rho_S \int S(\mathbf{r}^*) |\Psi^S_{\mathbf{k}^*}(\mathbf{r}^*)|^2 d^3\mathbf{r}^* \\
&\longrightarrow C(|\mathbf{k}^*|) \equiv C(k^*) = \sum_S \rho_S \langle |\Psi^S(\mathbf{k}^*_\mathbf{i}, \mathbf{r}^*_\mathbf{i})|^2 \rangle_i \\
&\longrightarrow C(k^*) = \lambda \sum_S \rho_S \langle |\Psi^S(\mathbf{k}^*_\mathbf{i}, \mathbf{r}^*_\mathbf{i})|^2 \rangle_i + (1-\lambda)
\end{aligned}
\tag{5}
$$

5.3 Momentum Resolution Corrections

Talk about Momentum resolution corrections

$$
C_{fit}(k^*_{Rec}) = \frac{\sum\limits_{k^*_{True}} M_{k^*_{Rec}, k^*_{True}} C_{fit}(k^*_{True})}{\sum\limits_{k^*_{True}} M_{k^*_{Rec}, k^*_{True}}} \tag{6}
$$

5.4 Residual Correlations

Talk about Lednicky model

6 Systematic Errors

This study is currently ongoing, and an estimate of my systematic uncertainties should be complete within a week. In order to understand my systematic uncertainties, the analysis code was run many times using slightly different values for a number of important cuts, and the results were compared. To quantify the effect, the difference in two correlation functions obtained using different values for a given cut was fit with a simple exponential decay function:

$$
\Delta C(k^*) = A e^{-Bk^*} \tag{7}
$$

The amplitude, A, and its associated uncertainty for the various cuts can be found in Tables 1 through 17. The systematic effect of the variation is marked as significant ("Sig" column) if the amplitude is not withih 2σ of 0. Although this proves qualitatively useful, these fits will likely not be used to quantify the systematic effects.

In order to quantify the systematic errors on the correlation functions, all correlations will be averaged, and the resulting variance will be taken as the systematic error. Similarly, the fit parameters extracted from all of these correlation functions will be averaged, and they resulting variances will be taken as the systematic errors for the fit parameters.

6.1 Systematic Errors: $\Lambda \mathrm{K}^0_S$

6.1.1 Particle and Pair Cuts

The cuts included in the systematic study, as well as the values used in the variations, are listed below. Note, the central value corresponds to that used in the analysis.

1. DCA $\Lambda(\bar{\Lambda})$: {4, 5, 6 mm}
2. DCA K^0_S: {2, 3, 4 mm}
3. DCA $\Lambda(\bar{\Lambda})$ Daughters: {3, 4, 5 mm}

DCA $\Lambda(\bar{\Lambda})$

Pair Type	Centrality	Fit Amplitudes					
		Amplitude	Error	Sig	Amplitude	Error	Sig
		4 vs 5 mm			5 vs 6 mm		
ΛK^0_S	0-10%	2.616e-04	2.840e-04	No	-5.282e-03	4.887e-03	No
	10-30%	-1.236e-03	1.568e-03	No	6.110e-05	1.457e-04	No
	30-50%	-4.664e-02	3.295e-02	No	-1.877e-01	7.037e-02	Yes
$\bar{\Lambda}K^0_S$	0-10%	-6.093e-05	3.827e-05	No	-9.599e-02	1.133e-01	No
	10-30%	-3.478e-05	1.983e-04	No	-2.846e-04	6.743e-04	No
	30-50%	-2.054e-02	2.609e-02	No	-3.701e-03	3.136e-03	No

Table 1: $\Lambda(\bar{\Lambda})K^0_S$ Analyses: DCA $\Lambda(\bar{\Lambda})$ caption

DCA K^0_S

Pair Type	Centrality	Fit Amplitudes					
		Amplitude	Error	Sig	Amplitude	Error	Sig
		2 vs 3 mm			3 vs 4 mm		
ΛK^0_S	0-10%	-1.149e-04	1.616e-04	No	1.495e-04	3.020e-04	No
	10-30%	2.336e-04	7.234e-05	Yes	-2.560e-03	2.270e-03	No
	30-50%	-7.966e-03	4.151e-03	No	-1.721e-02	6.245e-03	Yes
$\bar{\Lambda}K^0_S$	0-10%	6.657e-05	5.808e-04	No	7.037e-05	2.753e-05	Yes
	10-30%	-4.373e-04	3.529e-04	No	-4.653e-04	3.627e-04	No
	30-50%	-2.048e-03	1.296e-03	No	-2.871e-04	8.150e-04	No

Table 2: $\Lambda(\bar{\Lambda})K^0_S$ Analyses: DCA K^0_S caption

4. DCA K^0_S Daughters: {2, 3, 4 mm}
5. $\Lambda(\bar{\Lambda})$ Cosine of Pointing Angle: {0.9992, 0.9993, 0.9994}
6. K^0_S Cosine of Pointing Angle: {0.9992, 0.9993, 0.9994}
7. DCA to Primary Vertex of $p(\bar{p})$ Daughter of $\Lambda(\bar{\Lambda})$: {0.5, 1, 2 mm}
8. DCA to Primary Vertex of $\pi^-(\pi^+)$ Daughter of $\Lambda(\bar{\Lambda})$: {0.5, 1, 2 mm}
9. DCA to Primary Vertex of π^+ Daughter of K^0_S: {2, 3, 4 mm}
10. DCA to Primary Vertex of π^- Daughter of K^0_S: {2, 3, 4 mm}
11. Average Separation of Like-Charge Daughters: {5, 6, 7 cm}

6.1.2 Non-Flat Background

6.1.3 Fit Range

6.1.4 Normalization Range

6.1.5 Momentum Resolution Correction

6.2 Systematic Errors: $\Lambda K^{\pm}$

6.2.1 Particle and Pair Cuts

The cuts included in the systematic study, as well as the values used in the variations, are listed below. Note, the central value corresponds to that used in the analysis.

DCA $\Lambda(\bar{\Lambda})$ Daughters

Pair Type	Centrality	Fit Amplitudes					
		Amplitude	Error	Sig	Amplitude	Error	Sig
		3 vs 4 mm			4 vs 5 mm		
ΛK^0_S	0-10%	1.743e-05	3.776e-05	No	1.972e-04	2.813e-04	No
	10-30%	1.293e-04	7.761e-05	No	-8.925e-05	6.165e-05	No
	30-50%	-8.647e-02	9.120e-02	No	-5.097e-02	5.611e-02	No
$\bar{\Lambda}K^0_S$	0-10%	-8.539e-06	3.914e-05	No	5.936e-05	3.128e-05	No
	10-30%	1.001e-04	7.999e-05	No	-2.452e-04	2.952e-04	No
	30-50%	4.672e-05	1.859e-04	No	-1.423e-01	1.753e-01	No

Table 3: $\Lambda(\bar{\Lambda})K^0_S$ Analyses: DCA $\Lambda(\bar{\Lambda})$ Daughters

DCA K^0_S Daughters

Pair Type	Centrality	Fit Amplitudes					
		Amplitude	Error	Sig	Amplitude	Error	Sig
		2 vs 3 mm			3 vs 4 mm		
ΛK^0_S	0-10%	-1.383e-03	1.201e-03	No	-2.394e-03	2.528e-03	No
	10-30%	-1.199e-01	6.112e-02	No	-1.673e-03	1.620e-03	No
	30-50%	-1.397e-01	5.508e-02	Yes	-2.249e-03	3.303e-03	No
$\bar{\Lambda}K^0_S$	0-10%	-3.646e-03	2.561e-03	No	-4.246e-04	5.171e-04	No
	10-30%	1.800e-04	8.734e-05	Yes	-7.128e-04	9.398e-04	No
	30-50%	-2.813e-02	1.883e-02	No	-1.285e-02	9.463e-03	No

Table 4: $\Lambda(\bar{\Lambda})K^0_S$ Analyses: DCA K^0_S Daughters

$\Lambda(\bar{\Lambda})$ Cosine of Pointing Angle

Pair Type	Centrality	Fit Amplitudes					
		Amplitude	Error	Sig	Amplitude	Error	Sig
		0.9992 vs 0.9993			0.9993 vs 0.9994		
ΛK^0_S	0-10%	4.733e-03	2.311e-03	Yes	-7.459e-05	1.768e-04	No
	10-30%	5.201e-03	2.270e-03	Yes	-2.253e-05	7.593e-05	No
	30-50%	-6.078e-05	6.309e-05	No	5.494e-03	1.496e-03	Yes
$\bar{\Lambda}K^0_S$	0-10%	-2.031e-05	8.438e-07	Yes	-4.978e-05	6.433e-05	No
	10-30%	3.929e-04	2.778e-04	No	1.333e-04	2.362e-04	No
	30-50%	1.770e-03	6.120e-04	Yes	1.169e-04	7.436e-05	No

Table 5: $\Lambda(\bar{\Lambda})K^0_S$ Analyses: $\Lambda(\bar{\Lambda})$ Cosine of Pointing Angle

K^0_S Cosine of Pointing Angle

Pair Type	Centrality	Fit Amplitudes					
		Amplitude	Error	Sig	Amplitude	Error	Sig
		0.9992 vs 0.9993			0.9993 vs 0.9994		
ΛK^0_S	0-10%	-3.282e-04	4.102e-04	No	7.088e-04	3.667e-04	No
	10-30%	1.476e-03	2.082e-03	No	8.069e-03	3.961e-03	Yes
	30-50%	-3.150e-04	6.895e-04	No	5.057e-03	2.639e-03	No
$\bar{\Lambda}K^0_S$	0-10%	5.986e-04	4.487e-04	No	7.197e-04	7.865e-04	No
	10-30%	3.562e-03	1.378e-03	Yes	1.303e-03	1.067e-03	No
	30-50%	5.878e-02	8.703e-02	No	1.493e-04	1.017e-04	No

Table 6: $\Lambda(\bar{\Lambda})K^0_S$ Analyses: K^0_S Cosine of Pointing Angle

DCA to Primary Vertex of $p^+(\bar{p}^-)$ Daughter of $\Lambda(\bar{\Lambda})$

Pair Type	Centrality	Fit Amplitudes					
		Amplitude	Error	Sig	Amplitude	Error	Sig
		0.5 vs 1 mm			1 vs 2 mm		
ΛK^0_S	0-10%	0.000e+00	0.000e+00	No	-2.602e-03	2.525e-03	No
	10-30%	2.964e-07	1.165e-06	No	1.702e-04	9.110e-05	No
	30-50%	0.000e+00	0.000e+00	No	5.775e-03	7.524e-03	No
$\bar{\Lambda}K^0_S$	0-10%	0.000e+00	0.000e+00	No	-2.584e-04	4.464e-04	No
	10-30%	0.000e+00	0.000e+00	No	-3.469e-04	1.403e-04	Yes
	30-50%	0.000e+00	0.000e+00	No	-6.689e-04	1.232e-03	No

Table 7: $\Lambda(\bar{\Lambda})K^0_S$ Analyses: DCA to Primary Vertex of $p^+(\bar{p}^-)$ Daughter of $\Lambda(\bar{\Lambda})$

DCA to Primary Vertex of $\pi^-(\pi^+)$ Daughter of $\Lambda(\bar{\Lambda})$

Pair Type	Centrality	Fit Amplitudes					
		Amplitude	Error	Sig	Amplitude	Error	Sig
		2 vs 3 mm			3 vs 4 mm		
ΛK^0_S	0-10%	3.829e-05	1.846e-05	Yes	-4.781e-05	8.826e-05	No
	10-30%	1.498e-03	2.398e-03	No	4.245e+00	4.457e+01	No
	30-50%	3.751e-03	2.567e-03	No	6.001e-03	4.805e-03	No
$\bar{\Lambda}K^0_S$	0-10%	5.680e-05	1.816e-05	Yes	-3.516e-05	2.272e-05	No
	10-30%	1.539e-04	2.857e-04	No	-1.311e-04	4.871e-05	Yes
	30-50%	1.410e-03	1.734e-03	No	4.401e-02	1.349e-02	Yes

Table 8: $\Lambda(\bar{\Lambda})K^0_S$ Analyses: DCA to Primary Vertex of $\pi^-(\pi^+)$ Daughter of $\Lambda(\bar{\Lambda})$

DCA to Primary Vertex of π^+ Daughter of K^0_S

Pair Type	Centrality	Fit Amplitudes					
		Amplitude	Error	Sig	Amplitude	Error	Sig
		2 vs 3 mm			3 vs 4 mm		
ΛK^0_S	0-10%	-4.519e-05	2.636e-05	No	-8.563e-05	3.040e-05	Yes
	10-30%	-8.408e-03	7.107e-03	No	-4.274e-04	9.735e-04	No
	30-50%	2.064e-03	1.619e-03	No	1.274e-03	1.270e-03	No
$\bar{\Lambda}K^0_S$	0-10%	8.474e-04	1.271e-03	No	3.787e-04	3.383e-04	No
	10-30%	-7.583e-05	5.660e-05	No	-7.112e-03	1.605e-02	No
	30-50%	-6.532e-04	1.388e-04	Yes	3.770e-02	1.629e-02	Yes

Table 9: $\Lambda(\bar{\Lambda})K^0_S$ Analyses: DCA to Primary Vertex of π^+ Daughter of K^0_S

DCA to Primary Vertex of π^- Daughter of K^0_S

Pair Type	Centrality	Fit Amplitudes					
		Amplitude	Error	Sig	Amplitude	Error	Sig
		2 vs 3 mm			3 vs 4 mm		
ΛK^0_S	0-10%	-3.283e-04	4.184e-04	No	3.117e-04	2.151e-04	No
	10-30%	-7.208e-07	3.153e-04	No	2.858e-04	6.697e-04	No
	30-50%	4.434e-02	2.574e-02	No	2.761e-04	1.565e-04	No
$\bar{\Lambda}K^0_S$	0-10%	8.823e-05	2.701e-05	Yes	9.286e-02	1.113e-01	No
	10-30%	1.778e-04	5.686e-05	Yes	1.343e-03	1.986e-03	No
	30-50%	1.449e-04	1.368e-04	No	-1.887e-04	1.605e-04	No

Table 10: $\Lambda(\bar{\Lambda})K^0_S$ Analyses: DCA to Primary Vertex of π^- Daughter of K^0_S

Avgerage Separation of Like-Charge Daughters

Pair Type	Daughters		Centrality	Fit Amplitude					
				Amplitude	Error	Sig	Amplitude	Error	Sig
				5.0 vs 6.0 cm			6.0 vs 7.0 cm		
ΛK^0_S	p(Λ)	$\pi^+(K^0_S)$	0-10%	1.665e-05	2.087e-06	Yes	2.653e-04	1.739e-04	No
			10-30%	2.331e-05	4.563e-05	No	-1.713e-05	6.046e-06	Yes
			30-50%	4.333e-04	1.155e-04	Yes	7.198e-04	1.244e-04	Yes
ΛK^0_S	$\pi^-(\Lambda)$	$\pi^-(K^0_S)$	0-10%	7.361e-06	2.047e-06	Yes	-2.548e-05	2.467e-05	No
			10-30%	4.421e-05	3.105e-05	No	7.315e-04	1.322e-04	Yes
			30-50%	6.366e-05	5.813e-05	No	1.154e-04	8.695e-06	Yes
$\bar{\Lambda}K^0_S$	$\pi^+(\bar{\Lambda})$	$\pi^+(K^0_S)$	0-10%	8.888e-04	2.082e-04	Yes	-5.316e-06	3.826e-05	No
			10-30%	9.162e-04	2.614e-04	Yes	1.925e-05	6.041e-05	No
			30-50%	1.478e-04	4.676e-05	Yes	9.973e-05	6.549e-05	No
$\bar{\Lambda}K^0_S$	$\bar{p}^-(\bar{\Lambda})$	$\pi^-(K^0_S)$	0-10%	1.730e-04	1.161e-04	No	-2.798e-05	4.725e-05	No
			10-30%	1.579e-05	5.734e-05	No	-3.884e-07	6.028e-06	No
			30-50%	1.074e-04	3.781e-05	Yes	4.932e-04	2.440e-04	Yes

Table 11: $\Lambda(\bar{\Lambda})K^0_S$ Analyses: Avgerage Separation of Positive Daughters

DCA $\Lambda(\bar{\Lambda})$

Pair Type	Centrality	Fit Amplitudes					
		Amplitude	Error	Sig	Amplitude	Error	Sig
		4 vs 5 mm			5 vs 6 mm		
ΛK^+	0-10%	-1.200e-04	8.688e-05	No	2.534e-04	1.983e-04	No
	10-30%	-3.714e-05	1.986e-04	No	6.806e-02	7.932e-02	No
	30-50%	-5.383e-02	6.237e-02	No	-3.545e-04	4.265e-04	No
$\bar{\Lambda}K^-$	0-10%	-1.388e-04	1.057e-04	No	4.615e-05	1.693e-05	Yes
	10-30%	-7.745e-04	4.039e-04	No	-3.957e-05	5.462e-04	No
	30-50%	1.601e-03	1.398e-03	No	2.435e-04	1.118e-03	No
ΛK^-	0-10%	-6.034e-05	1.158e-04	No	1.924e-03	1.398e-03	No
	10-30%	4.468e-05	4.450e-05	No	-4.520e-04	3.092e-04	No
	30-50%	-1.496e-03	9.168e-04	No	-7.476e-04	1.012e-03	No
$\bar{\Lambda}K^+$	0-10%	-1.777e-04	2.999e-04	No	-2.152e-05	1.639e-05	No
	10-30%	-3.655e-04	3.734e-04	No	-8.857e-04	7.247e-04	No
	30-50%	-1.650e-03	1.124e-03	No	-3.706e-04	3.366e-04	No

Table 12: $\Lambda(\bar{\Lambda})K^{\pm}$ Analyses: DCA $\Lambda(\bar{\Lambda})$

1. DCA $\Lambda(\bar{\Lambda})$: {4, 5, 6 mm}
2. DCA $\Lambda(\bar{\Lambda})$ Daughters: {3, 4, 5 mm}
3. $\Lambda(\bar{\Lambda})$ Cosine of Pointing Angle: {0.9992, 0.9993, 0.9994}
4. DCA to Primary Vertex of $p(\bar{p})$ Daughter of $\Lambda(\bar{\Lambda})$: {0.5, 1, 2 mm}
5. DCA to Primary Vertex of $\pi^-(\pi^+)$ Daughter of $\Lambda(\bar{\Lambda})$: {0.5, 1, 2 mm}
6. Average Separation of $\Lambda(\bar{\Lambda})$ Daughter with Same Charge as $K^{\pm}$: {7, 8, 9 cm}

DCA $\Lambda(\bar{\Lambda})$ Daughters

Pair Type	Centrality	Fit Amplitudes					
		Amplitude	Error	Sig	Amplitude	Error	Sig
		3 vs 4 mm			4 vs 5 mm		
ΛK^+	0-10%	-1.170e-02	9.437e-03	No	-2.349e-03	1.142e-03	Yes
	10-30%	-3.522e-04	3.863e-04	No	1.359e-05	3.543e-05	No
	30-50%	1.090e-03	1.354e-03	No	-7.623e-02	3.708e-02	Yes
$\bar{\Lambda}K^-$	0-10%	-1.306e-04	1.486e-04	No	-4.771e-04	5.081e-04	No
	10-30%	7.482e-04	8.811e-04	No	8.166e-05	3.779e-05	Yes
	30-50%	-7.928e-04	1.146e-03	No	-2.568e-04	8.664e-05	Yes
ΛK^-	0-10%	-1.498e-04	1.562e-04	No	-5.849e-04	6.665e-04	No
	10-30%	1.204e-05	2.583e-04	No	-9.794e-05	1.314e-04	No
	30-50%	-9.314e-03	6.614e-03	No	-1.264e-04	8.487e-05	No
$\bar{\Lambda}K^+$	0-10%	-4.149e-04	3.296e-04	No	5.288e-05	7.505e-05	No
	10-30%	2.293e-04	3.396e-04	No	-8.853e-04	1.196e-03	No
	30-50%	-6.129e-05	7.969e-04	No	1.735e-04	8.784e-05	No

Table 13: $\Lambda(\bar{\Lambda})K^{\pm}$ Analyses: DCA $\Lambda(\bar{\Lambda})$ Daughters

$\Lambda(\bar{\Lambda})$ Cosine of Pointing Angle

Pair Type	Centrality	Fit Amplitudes					
		Amplitude	Error	Sig	Amplitude	Error	Sig
		0.9992 vs 0.9993			0.9993 vs 0.9994		
ΛK^+	0-10%	-1.448e-05	9.361e-06	No	6.215e-04	4.967e-04	No
	10-30%	3.355e-02	2.063e-02	No	5.291e-04	7.270e-04	No
	30-50%	4.609e-03	5.410e-03	No	1.360e-04	4.949e-05	Yes
$\bar{\Lambda}K^-$	0-10%	-4.085e-06	1.016e-05	No	1.211e-05	1.145e-05	No
	10-30%	1.249e-04	1.660e-04	No	-2.328e-05	2.350e-05	No
	30-50%	2.214e-03	1.301e-03	No	-3.532e-03	4.294e-03	No
ΛK^-	0-10%	3.409e-05	9.589e-06	Yes	1.170e-04	1.430e-04	No
	10-30%	6.537e-05	1.967e-05	Yes	2.119e-04	2.609e-04	No
	30-50%	-4.434e-05	4.608e-05	No	9.610e-05	5.145e-05	No
$\bar{\Lambda}K^+$	0-10%	-3.270e-05	5.714e-05	No	-1.744e-05	1.103e-05	No
	10-30%	-7.203e-05	2.042e-05	Yes	1.023e-04	1.924e-04	No
	30-50%	2.030e-03	1.831e-03	No	7.645e-05	5.303e-05	No

Table 14: $\Lambda(\bar{\Lambda})K^{\pm}$ Analyses: $\Lambda(\bar{\Lambda})$ Cosine of Pointing Angle

DCA to Primary Vertex of $p^+(\bar{p}^-)$ Daughter of $\Lambda(\bar{\Lambda})$

Pair Type	Centrality	Fit Amplitudes					
		Amplitude	Error	Sig	Amplitude	Error	Sig
		0.5 vs 1 mm			1 vs 2 mm		
ΛK^+	0-10%	0.000e+00	0.000e+00	No	-2.429e-04	2.561e-04	No
	10-30%	-3.554e-08	6.097e-08	No	1.598e-04	7.738e-05	Yes
	30-50%	0.000e+00	0.000e+00	No	-2.317e-03	1.992e-03	No
$\bar{\Lambda}K^-$	0-10%	0.000e+00	0.000e+00	No	-9.883e-04	9.265e-04	No
	10-30%	0.000e+00	0.000e+00	No	-2.472e-04	5.419e-04	No
	30-50%	0.000e+00	0.000e+00	No	1.227e-03	1.328e-03	No
ΛK^-	0-10%	0.000e+00	0.000e+00	No	3.677e-03	4.028e-03	No
	10-30%	1.875e-07	1.095e-06	No	6.518e-03	5.373e-03	No
	30-50%	0.000e+00	0.000e+00	No	-2.985e-04	5.747e-04	No
$\bar{\Lambda}K^+$	0-10%	0.000e+00	0.000e+00	No	-4.252e-04	3.414e-04	No
	10-30%	0.000e+00	0.000e+00	No	1.033e-03	8.146e-04	No
	30-50%	0.000e+00	0.000e+00	No	-7.193e-04	7.376e-04	No

Table 15: $\Lambda(\bar{\Lambda})K^{\pm}$ Analyses: DCA to Primary Vertex of $p^+(\bar{p}^-)$ Daughter of $\Lambda(\bar{\Lambda})$

DCA to Primary Vertex of $\pi^-(\pi^+)$ Daughter of $\Lambda(\bar{\Lambda})$

Pair Type	Centrality	Fit Amplitudes					
		Amplitude	Error	Sig	Amplitude	Error	Sig
		2 vs 3 mm			3 vs 4 mm		
ΛK^+	0-10%	7.991e-02	3.641e-01	No	-2.774e-03	3.759e-03	No
	10-30%	-2.559e-05	5.097e-05	No	-4.152e-03	3.267e-03	No
	30-50%	1.461e-02	5.067e-03	Yes	-8.144e-05	3.055e-04	No
$\bar{\Lambda}K^-$	0-10%	-9.069e-06	1.070e-05	No	-1.506e-04	2.900e-04	No
	10-30%	1.485e-05	2.273e-05	No	-2.281e-04	2.219e-04	No
	30-50%	3.830e-03	2.477e-03	No	-2.258e-04	8.241e-04	No
ΛK^-	0-10%	-4.017e-05	5.473e-05	No	-3.418e-05	5.661e-05	No
	10-30%	6.474e-05	7.444e-05	No	4.487e-04	6.332e-04	No
	30-50%	3.344e-03	3.224e-03	No	9.751e-05	7.055e-05	No
$\bar{\Lambda}K^+$	0-10%	2.080e-05	1.035e-05	Yes	-1.947e-05	9.814e-05	No
	10-30%	-4.528e-04	3.642e-04	No	6.138e-05	2.809e-05	Yes
	30-50%	2.643e-04	5.272e-05	Yes	-2.107e-03	1.815e-03	No

Table 16: $\Lambda(\bar{\Lambda})K^{\pm}$ Analyses: DCA to Primary Vertex of $\pi^-(\pi^+)$ Daughter of $\Lambda(\bar{\Lambda})$

Average Separation of $\Lambda(\bar{\Lambda})$ Daughter With Same Charge as $K^{\pm}$

Pair Type	Daughter	Track	Centrality	Fit Amplitudes					
				Amplitude	Error	Sig	Amplitude	Error	Sig
				7 vs 8 mm			8 vs 9 mm		
ΛK^{+}	p(Λ)	K^{+}	0-10%	1.310e-06	1.696e-07	Yes	4.374e-06	2.246e-07	Yes
			10-30%	2.084e-06	4.698e-07	Yes	4.124e-06	4.593e-06	No
			30-50%	-1.186e-03	9.739e-04	No	3.110e-05	3.395e-05	No
$\bar{\Lambda}K^{-}$	$\bar{p}^{-}(\bar{\Lambda})$	K^{-}	0-10%	2.057e-06	1.499e-07	Yes	3.829e-06	1.327e-07	Yes
			10-30%	7.002e-06	6.292e-06	No	4.608e-06	4.256e-06	No
			30-50%	4.608e-06	4.256e-06	No	9.199e-05	7.119e-05	No
ΛK^{-}	$\pi^{-}(\Lambda)$	K^{-}	0-10%	4.686e-06	3.491e-07	Yes	2.311e-06	5.498e-07	Yes
			10-30%	5.411e-06	7.471e-07	Yes	7.344e-06	5.583e-07	Yes
			30-50%	2.045e-04	1.593e-04	No	1.570e-04	3.330e-04	No
$\bar{\Lambda}K^{+}$	$\pi^{+}(\bar{\Lambda})$	K^{+}	0-10%	-3.063e-04	1.137e-04	Yes	-6.134e-05	6.307e-05	No
			10-30%	6.019e-06	6.879e-07	Yes	1.473e-06	1.292e-06	No
			30-50%	1.773e-04	6.857e-05	Yes	1.701e-04	1.120e-04	No

Table 17: $\Lambda(\bar{\Lambda})K^{0}_{S}$ Analyses: Average Separation of $\Lambda(\bar{\Lambda})$ Daughter With Same Charge as $K^{\pm}$

6.2.2 Non-Flat Background

6.2.3 Fit Range

6.2.4 Normalization Range

6.2.5 Momentum Resolution Correction

7 Results and Discussion

8 To Do

References

[1] Michael Annan Lisa, Scott Pratt, Ron Soltz, and Urs Wiedemann. Femtoscopy in relativistic heavy ion collisions. *Ann. Rev. Nucl. Part. Sci.*, 55:357–402, 2005.

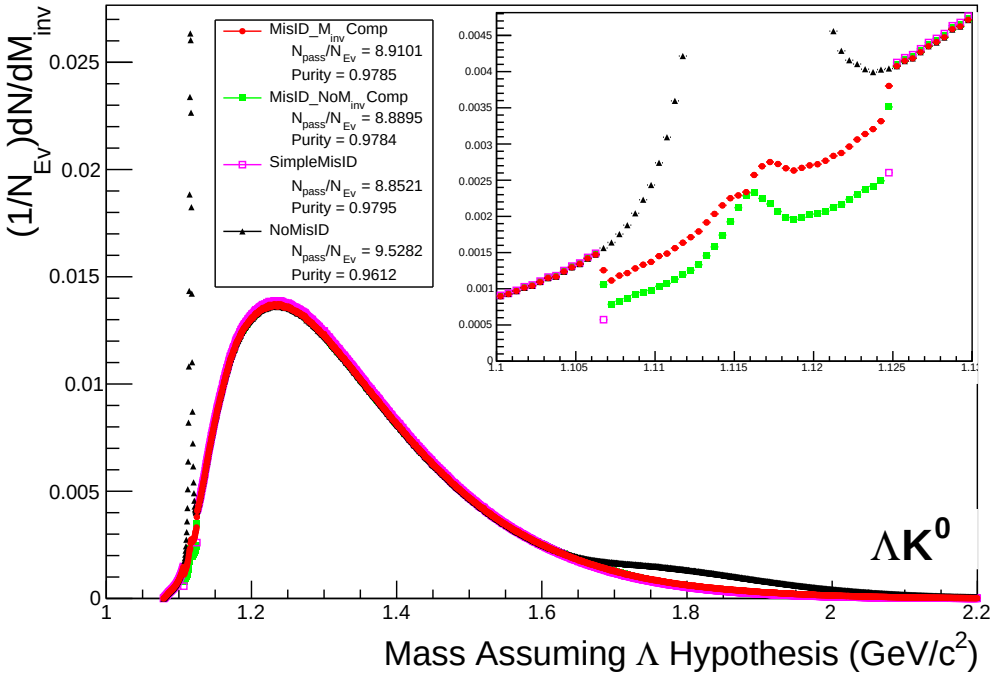

(a) Mass assuming Λ-hypothesis for K^0_S collection, i.e. assume the daughters are $p^+\pi^-$ instead of $\pi^+\pi^-$.

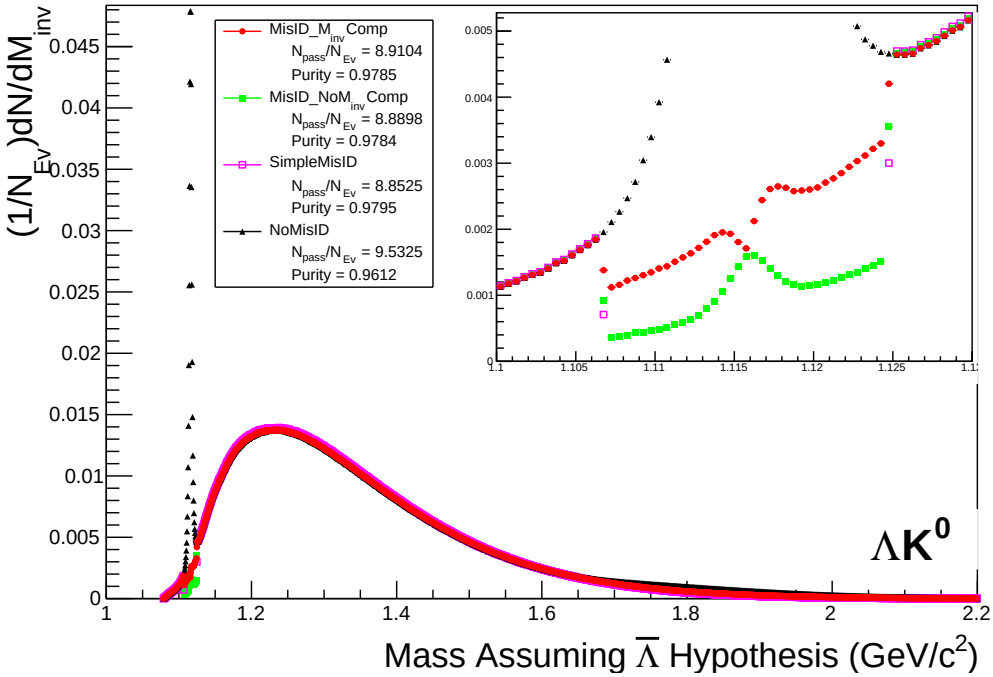

(b) Mass assuming $\bar{\Lambda}$-hypothesis for K^0_S collection, i.e. assume the daughters are $\pi^+\bar{p}^-$ instead of $\pi^+\pi^-$.

Fig. 4: Mass assuming Λ-hypothesis (4a) and $\bar{\Lambda}$-hypothesis (4b) for K^0_S collection. The "NoMisID" distribution (black triangles) uses the V0 finder without any attempt to remove misidentified Λ and $\bar{\Lambda}$. The peak in the "NoMisID" distribution around $m_{inv} = 1.115$ GeV/c^2 contains misidentified Λ (4a) and $\bar{\Lambda}$ (4b) particles in our K^0_S collection. "SimpleMisID" (pink squares) simply cuts out the entire peak, which throws away some good K^0_S particles. "MisID_NoM$_{inv}$Comp" (green squares) uses the misidentification cut outlined in the text, but does not utilize the invariant mass comparison method. "MisID_M$_{inv}$Comp" (red circles) utilizes the full misidentification methods, and is currently used for this analysis. "N$_{pass}$/N$_{ev}$" is the total number of K^0_S particles found, normalized by the total number of events. The purity of the collection is also listed. Also note, the relative excess of the "NoMisID" distribution around $1.65 < m_{inv} < 2.1$ GeV/c^2 shows misidified $\bar{\Lambda}$ (4a) and Λ (4b) particles in our K^0_S collection.

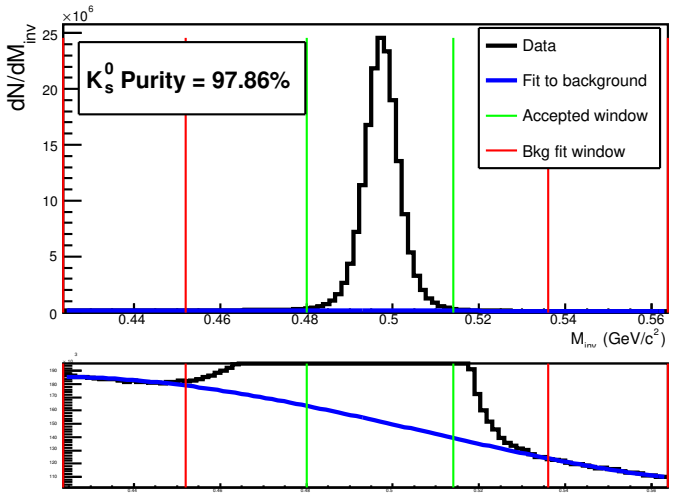

Fig. 5: Invariant mass (M_{inv}) distribution of all K^0_S candidates immediately before the final invariant mass cut. This distribution is used to calculate the collection purity, Purity(K^0_S) $\approx 98\%$.

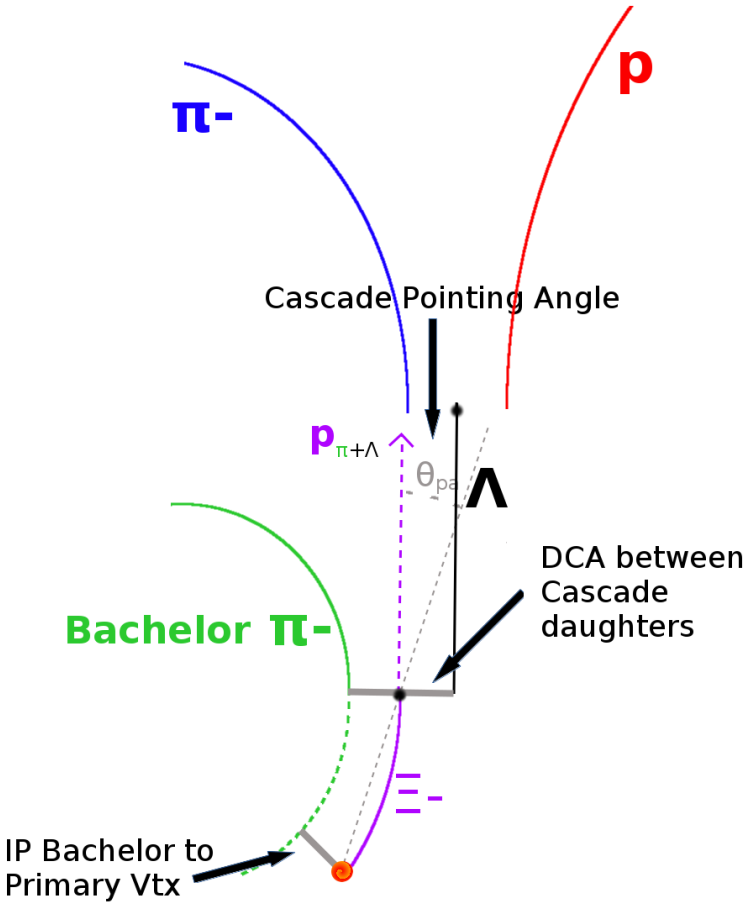

Fig. 6: Ξ Reconstruction

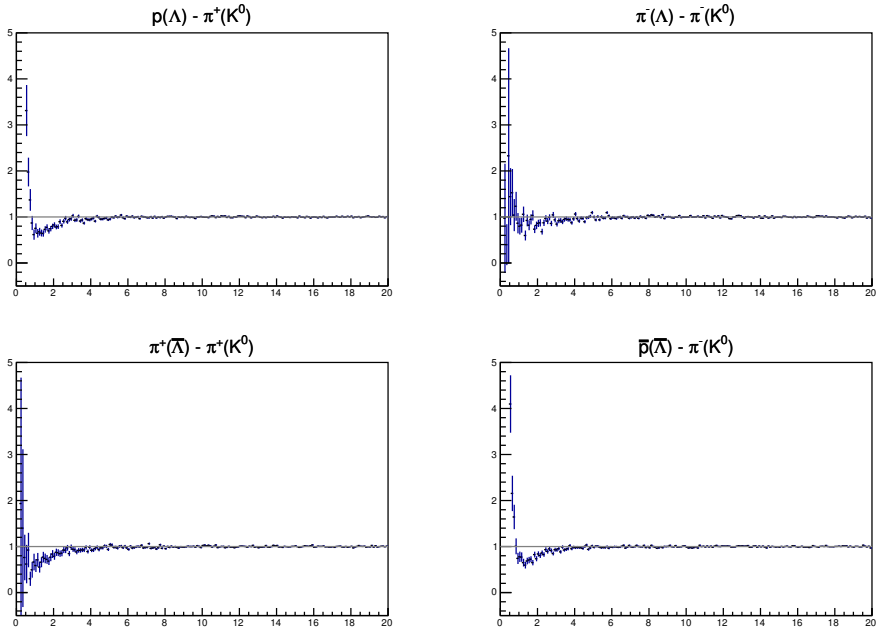

Fig. 7: Avgerage Separation of $\Lambda(\bar{\Lambda})$ and K^0_S Daughters. Only like-sign daughter pairs are shown (the distributions for unlike-signs were found to be flat). The title of each subfigure shows the daughter pair, as well as the mother of each daughter (in "()"), ex. top left is p from Λ with π^+ from K^0_S.

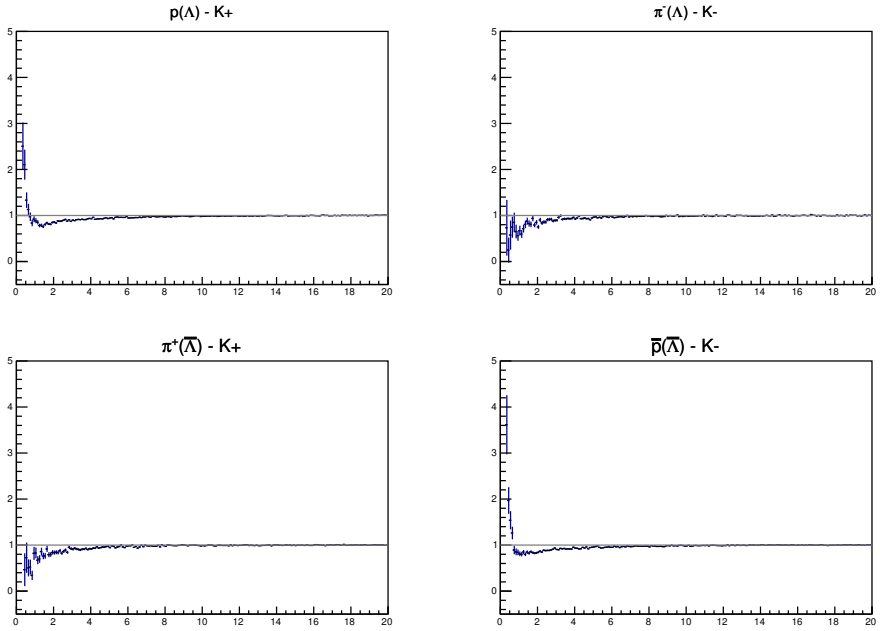

Fig. 8: Avgerage Separation of $\Lambda(\bar{\Lambda})$ Daughter and $K^{\pm}$. Only like-sign pairs are shown (unlike-signs were flat). In the subfigure titles, the particles in "()" represent the mothers, ex. top left is p from Λ with K^+.

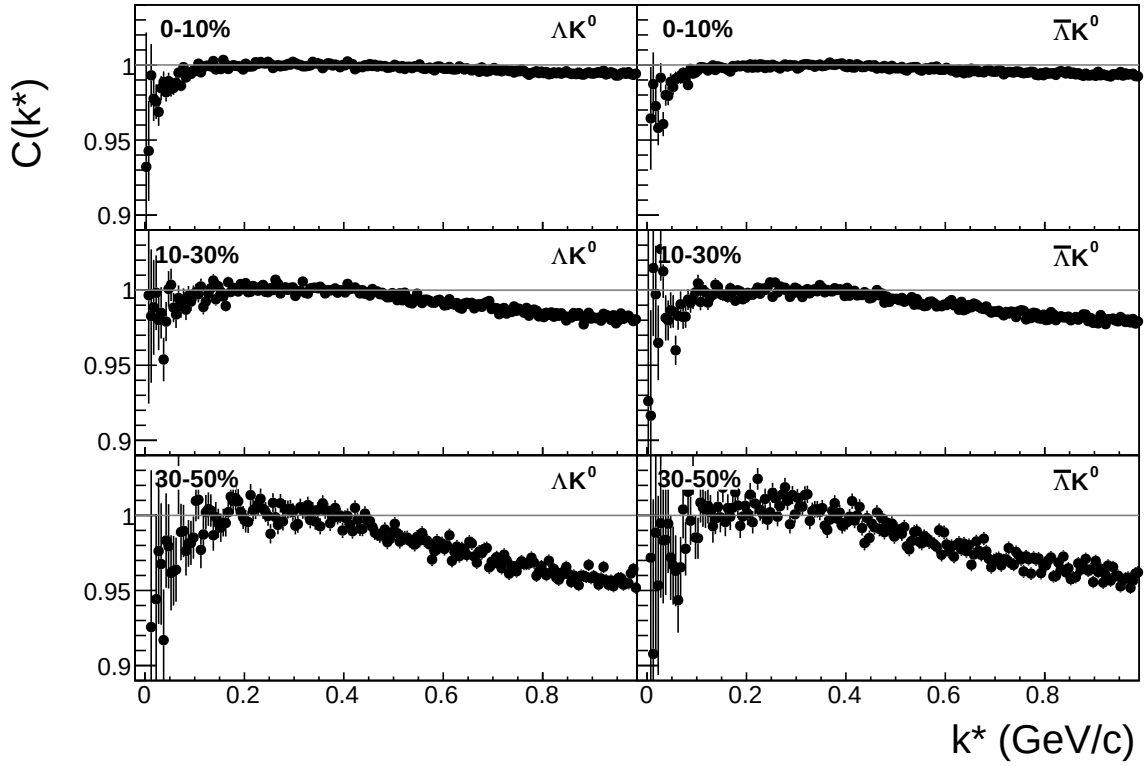

Fig. 9: ΛK^0_S (left) and $\bar{\Lambda} K^0_S$ (right) correlation functions for 0-10% (top), 10-30%(middle), and 30-50%(bottom) centralities.

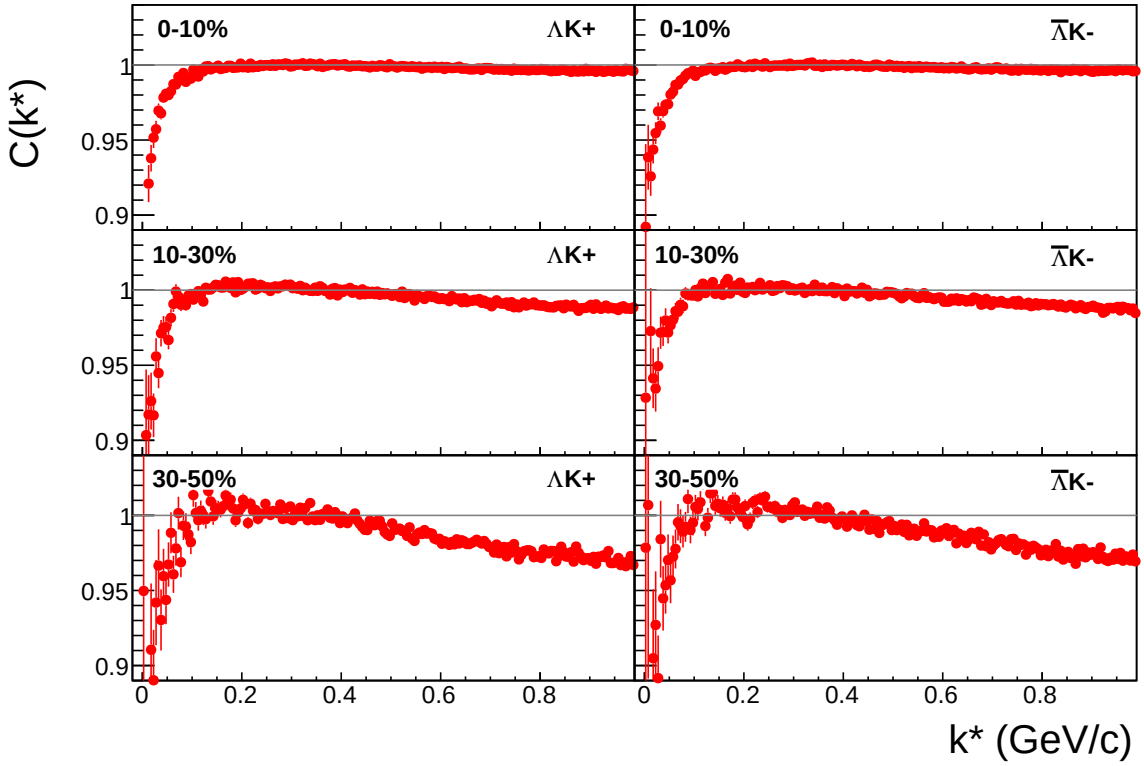

Fig. 10: ΛK^+ (left) and $\bar{\Lambda} K^-$ (right) correlation functions for 0-10% (top), 10-30%(middle), and 30-50%(bottom) centralities.

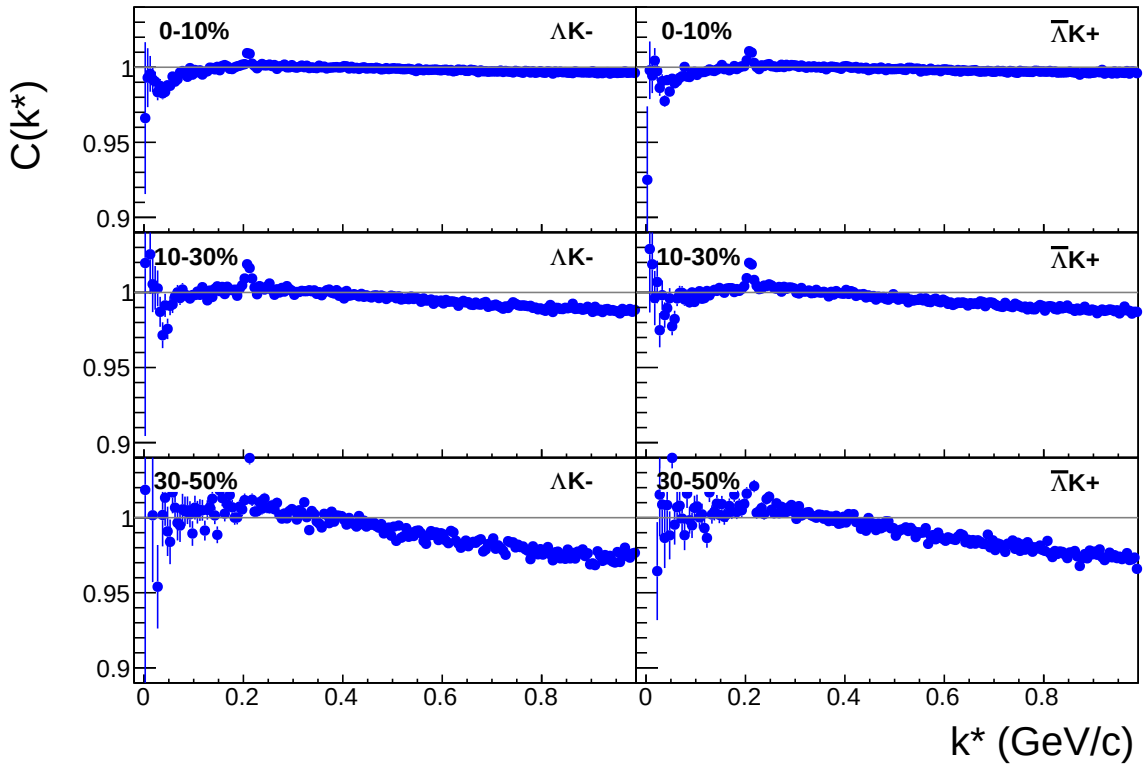

Fig. 11: ΛK^- (left) and $\bar{\Lambda}K^+$ (right) correlation functions for 0-10% (top), 10-30%(middle), and 30-50%(bottom) centralities. The peak at k* $\approx$ 0.2 GeV/c is due to the Ω^- resonance.

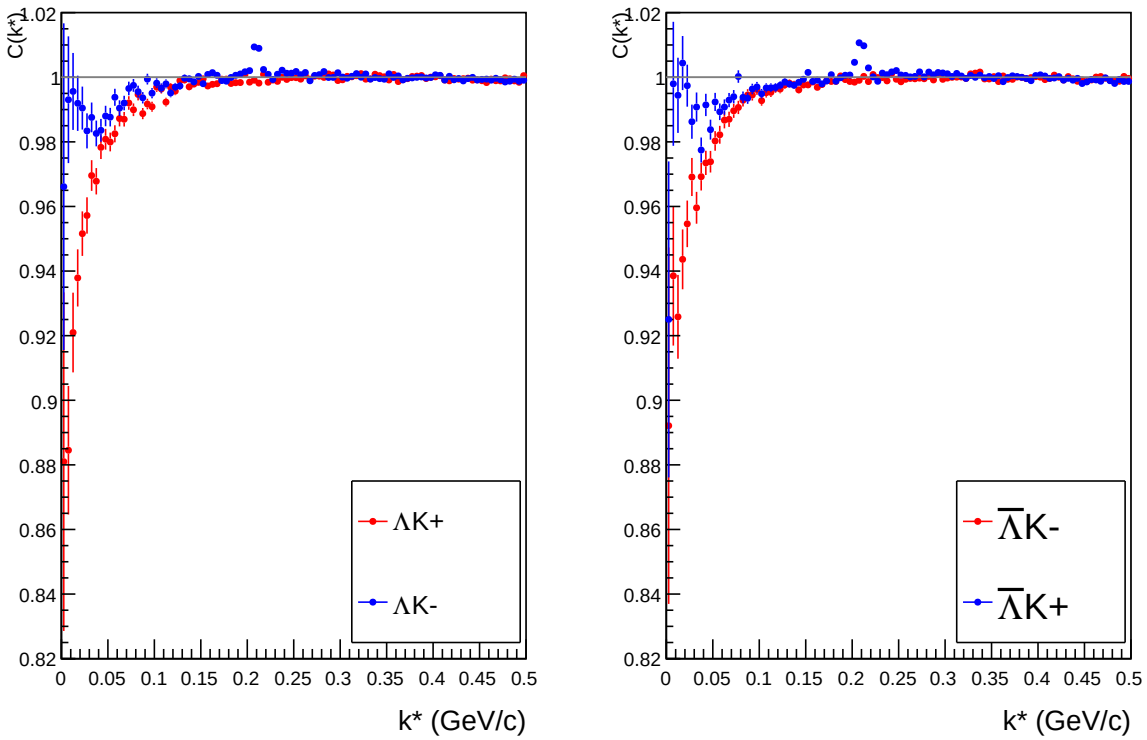

Fig. 12: Correlation Functions: ΛK^+ vs ΛK^- ($\bar{\Lambda} K^+$ vs $\bar{\Lambda} K^-$) for 0-10% centrality. The peak in ΛK^-($\bar{\Lambda} K^+$) at k* $\approx$ 0.2 GeV/c is due to the Ω^- resonance.

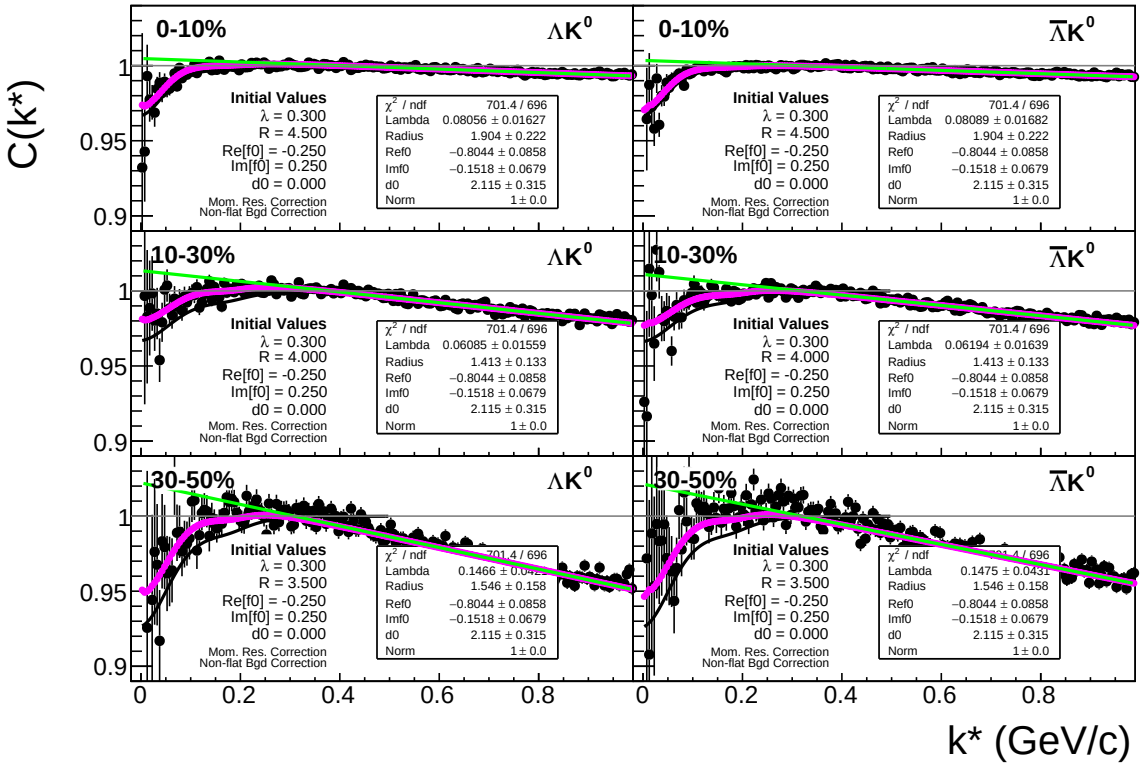

Fig. 13: $\Lambda K^0_S(\bar{\Lambda}K^0_S)$ Fits

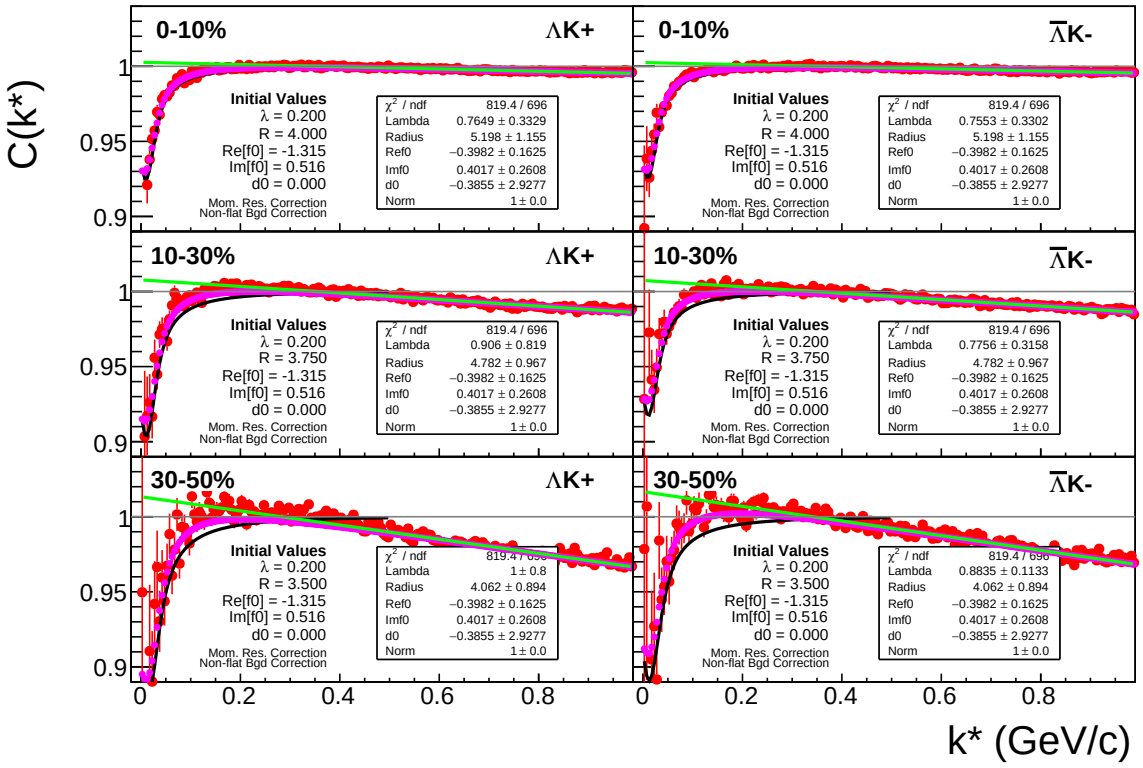

Fig. 14: $\Lambda K^+(\bar{\Lambda}K^-)$ Fits

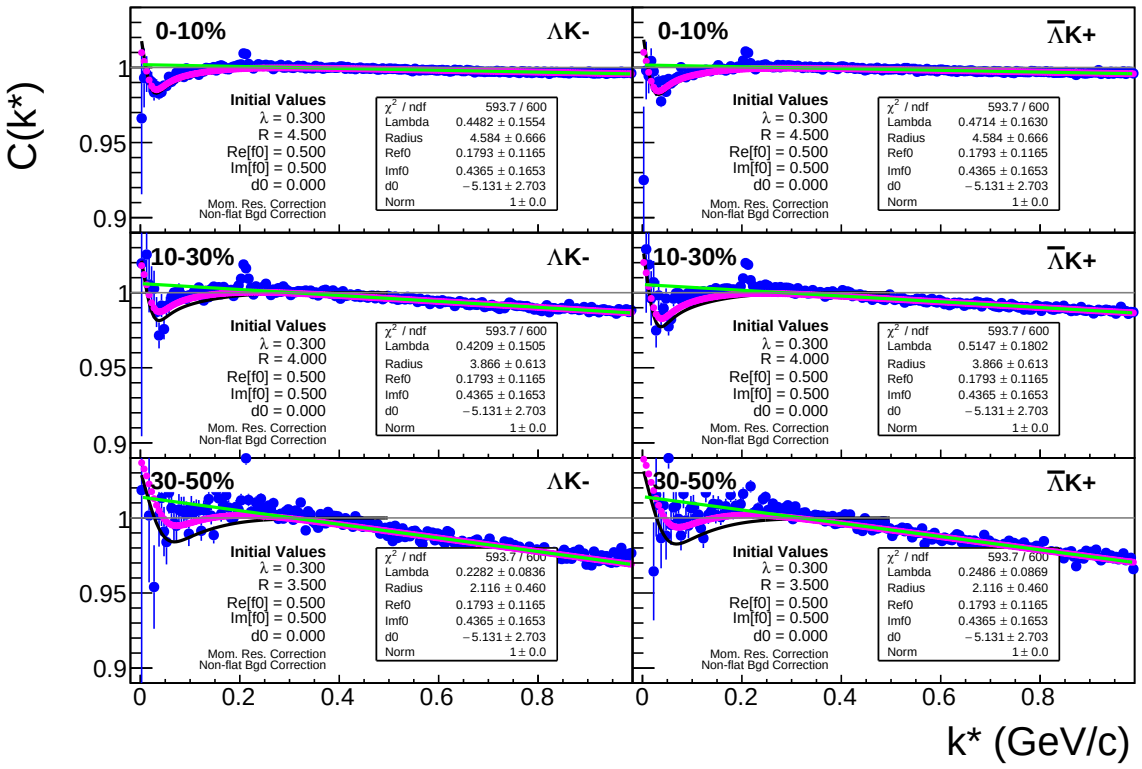

Fig. 15: $\Lambda K^{-}(\bar{\Lambda}K^{+})$ Fits